Effect of Hydrogen Bonding on the Spin Density Distribution and Hyperfine Couplings of the *p*-Benzosemiquinone Anion Radical in Alcohol Solvents: A Hybrid Density Functional Study

Patrick J. O'Malley

Department of Chemistry, UMIST, Manchester, M60 1QD, England

Received: September 15, 1997[⊗]

Hybrid density functional calculations utilizing the B3LYP functional are used to calculate geometries, spin densities, and isotropic and anisotropic hyperfine couplings for the *p*-benzosemiquinone anion radical. Hydrogen-bonding interactions with methanol, ethanol, 2-propanol, and water are studied for their effects on the above properties. A redistribution of unpaired electron spin density from the oxygen and ring carbon atom positions to the carbonyl carbon atom position is shown to occur on hydrogen bond formation. Outstanding agreement between calculated and experimental hyperfine couplings is observed.

Introduction

Quinones are ubiquitous to living systems and represent important cofactors for electron transfer in photosynthesis and respiration.[1] In photosynthesis, for example, quinones act as electron acceptors in the initial charge separation. For both bacterial and higher plant photosystem 2, two quinones termed Q_a and Q_b act in concert to enable efficient charge separation to take place.[2] Q_a is initially reduced to form the semiquinone anion radical. This then forwards its electron to Q_b, forming the Q_b semiquinone anion radical. On further charge separation Q_a accepts another electron to form the semiquinone anion radical again. This electron is then passed on to the already reduced Q_b, resulting in quinol, QH_2, formation, which leaves the protein site to be replaced by another quinone molecule from a quinone pool nearby.

Q_a and Q_b are often identical quinones: plastoquinone in higher plants and ubiquinone in bacterial systems. Their differing functions and properties are therefore conferred by their interactions with their protein environment. A variety of spectroscopic methods, most notably EPR, ENDOR, FTIR, and NMR, have been used to investigate such differences.[3−5] Differences in the hydrogen-bonding ability of both quinones are generally put forward for the differing functions observed; that is, specific hydrogen bonds to nearby amino acid residues are able to tailor the quinone to perform a specific function.

In this study we use modern density functional methods to examine the structure, spin density distribution, and hyperfine couplings of the parent semiquinone anion, *p*-benzosemiquinone anion radical, in various hydrogen-bonding solvents. First-principles electronic structure methods provide a unique probe into the electronic influence of hydrogen bonding on the electronic structure of quinones and their semiquinone anion forms. It is imperative to perform an in-depth study of the parent unsubstituted form initially to investigate the key electronic structure factors which change on hydrogen bond formation. Hydrogen-bonding complexes with water, methanol, ethanol, and 2-propanol are studied. The influence of hydrogen bonding on spin densities and isotropic and anisotropic hyperfine couplings is primarily studied.

Hybrid density functional methods, particularly the B3LYP functional, are increasingly being shown to provide excellent electronic structures for nonradicals and radicals alike.[6−8] They are uniquely capable of giving highly accurate descriptions of free radical properties such as isotropic and anisotropic hyperfine coupling constants.[8,9] For free radical properties Hartree−Fock-based methods perform very poorly.[9] Nuclear hyperfine couplings consist of an isotropic (Fermi contact) and anisotropic (dipolar) terms. In the electronic structure calculation both are calculated separately. Experimentally, in liquid solution, rapid tumbling leads to the elimination of the anisotropic components, and the isotropic value is obtained in isolation. For solid-state studies both the isotropic and anisotropic terms contribute to the coupling, and the total tensor is the experimental observable.

For calculation purposes the 3×3 hyperfine interaction tensor can be separated into its isotropic (spherically symmetric) and anisotropic (dipolar) components. To first order isotropic hyperfine interactions, $A_{iso}(N)$, are related to the spin densities, $\rho^s(r_N)$, at the corresponding nuclei by

$$A_{iso}(N) = (8\pi/3) g_e g_N \beta\beta_N \rho^s(r_N)$$

The anisotropic components are derived from the classical expression of interacting dipoles:

$$T_{ij}(N) = g_e g_N \beta\beta_N \sum P^{\alpha-\beta}{}_{\mu\nu} \langle \varphi_\mu | r^{-5}{}_{kN} (r^2{}_{kN}\delta_{ij} - 3 r_{kNi} r_{kNj}) | \varphi_\nu \rangle$$

β, β_N are the electron and nuclear magnetons and g_e, g_N the electron and nuclear magnetogyric ratios, respectively.

The isotropic component can be obtained form the Fermi contact analysis given by most modern electronic structure programs. The anisotropic components can be obtained from the spin only electric field gradient tensors.

Methods

The *p*-benzosemiquinone anion radical (BQ^-) is shown in Figure 1 together with the numbering scheme used hydrogen-bonded complexes with four water (BQ^-/WATER), methanol (BQ^-/METHANOL), ethanol (BQ^-/ETHANOL), and 2-propanol (BQ^-/IP) molecules, Figures 2 and 3 were used to model hydrogen-bonding interactions. Two conformations for the hydrogen bond interaction were used: an eclipsed form, A, Figure 2, and a staggered form, B, Figure 3.

All studies utilized the Becke3 exchange functional combined with the Lee, Yang, Parr correlation functional, B3LYP,[10] as implemented on GAUSSIAN94.[11] The calculations used the double-ζ EPR-II[9] basis set and were performed using GAUSS-

[⊗] Abstract published in *Advance ACS Abstracts,* November 15, 1997.

S1089-5639(97)03032-6 CCC: $14.00

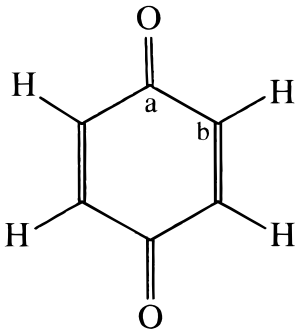

Figure 1. Structure and labeling of *p*-benzosemiquinone, BQ^-.

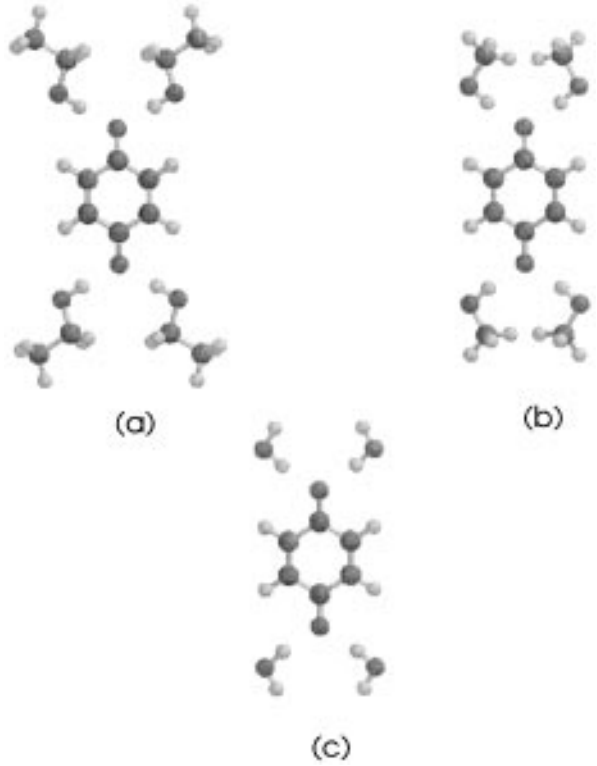

Figure 2. Structure of complexes studied, A conformers: (a) BQ^-/ETHANOL_A, (b) BQ_/METHANOL_A, (c) BQ^-/WATER_A. All D_{2h} point group symmetry.

IAN 94.[11] The appropriateness of the EPR-II basis set for hyperfine coupling calculations has been recently investigated by us.[8] Graphical representations of spin densities were generated using SPARTAN.[12] The calculations were run on DEC and Silicon Graphics workstations.

Results and Discussion

(a) Geometry. The calculated hydrogen bond distances for the semiquinone hydrogen bond complexes are given in Table 1. No major changes are brought about on the internal geometry of the *p*-benzosemiquinone molecule as a result of hydrogen bond formation. Changing the conformation of the hydrogen-bonding water or alcohol molecule does cause some changes in the hydrogen-bonding distance. In general the eclipsed, or

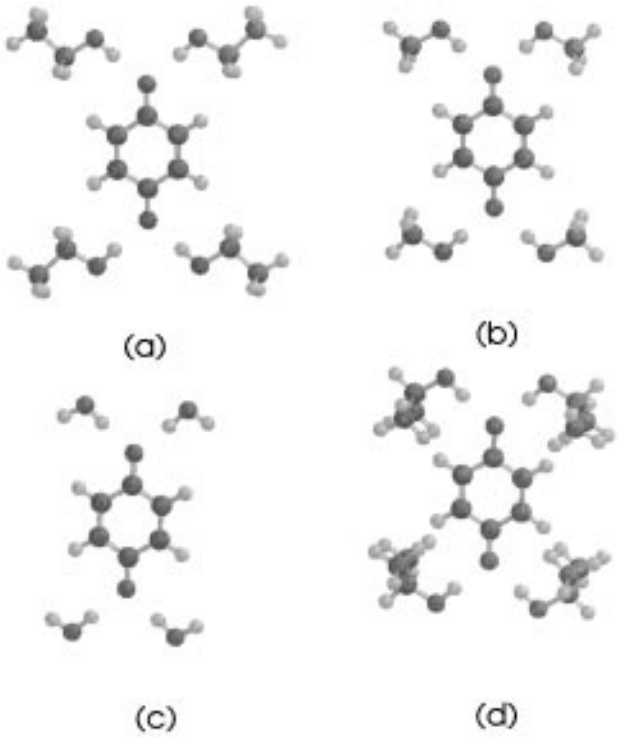

Figure 3. Structure of complexes studied, B conformers: (a) BQ^-/ETHANOL_B, (b) BQ^-/METHANOL_B, (c) BQ^-/WATER_B, (d) BQ^-/IP_B. All D_{2h} point group symmetry.

A, conformations have shorter intermolecular hydrogen bonds than the B conformers: see Table 1. For the water, methanol, and ethanol complexes the A conformer was the lowest energy structure. For the 2-propanol complex only the B conformer was stable due to steric crowding of the A form.

(b) Unpaired Spin Densities. Unpaired spin density plots for BQ^- and BQ^-/ETHANOL_A are shown in Figure 4. The 0.01 e/au^3 plot shows that the unpaired spin is concentrated at the O atoms with smaller amounts appearing at the C_a and C_b positions. From Figure 4 we can see that hydrogen bonding leads to an increase in spin density at the C_a position. The effect of hydrogen bonding on the unpaired spin density distribution is more clearly demonstrated by the unpaired spin density difference plots, BQ^-/ETHANOL_A$-BQ^-$, of Figure 5. Here we can see that hydrogen bonding leads to an increase in the unpaired spin density at the C_a position, positive difference plot, Figure 5a. The negative spin density difference plot, Figure 5b, demonstrates that this increase in unpaired spin density at C_a occurs at the expense of a decrease at the O (primarily) and the C_b position. In essence therefore hydrogen bonding leads to a redistribution of π electron unpaired spin density from the O and C_b atom positions to the C_a atom position. A similar redistribution of unpaired spin density on hydrogen bond formation is observed for all other solvents studied.

(c) Isotropic and Anisotropic Hyperfine Couplings. The isotropic, anisotropic and total(isotropic plus anisotropic) hyperfine couplings calculated for BQ^- and BQ^-/ETHANOL_A are given in Table 2. The major changes to hyperfine couplings are brought about on going from the isolated to the hydrogen-

TABLE 1: UB3LYP/EPR−II Calculated Bond Distances (Å) for the Complexes of Figures 2 and 3

bond	BQ^-/ ETHANOL_A	BQ^-/ ETHANOL_B	BQ^-/ METHANOL_A	BQ^-/ METHANOL_B	BQ^-/ WATER_A	BQ^-/ WATER_B	BQ^-/ IP_B
C_a-O	1.29	1.28	1.29	1.28	1.29	1.28	1.28
C_a-C_b	1.45	1.45	1.45	1.45	1.45	1.45	1.45
C_b-C_b	1.38	1.38	1.38	1.38	1.38	1.38	1.38
O−H(hb)	1.75	1.80	1.75	1.81	1.78	1.83	1.87

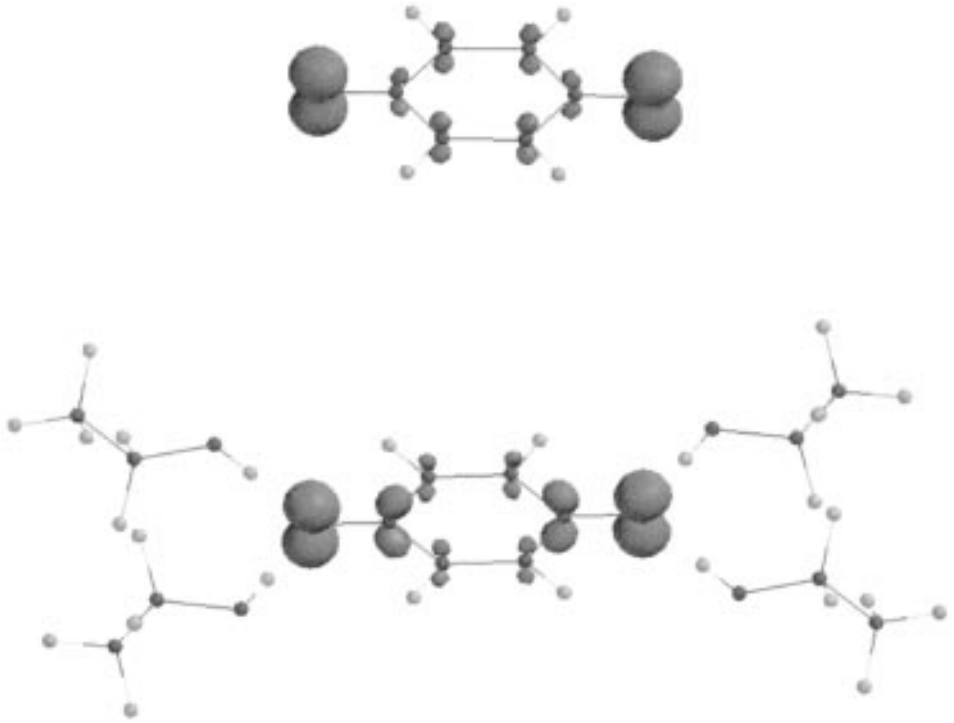

Figure 4. 0.01 e/au^3 contoured unpaired spin density plots for BQ^- and BQ^-/ETHANOL_A.

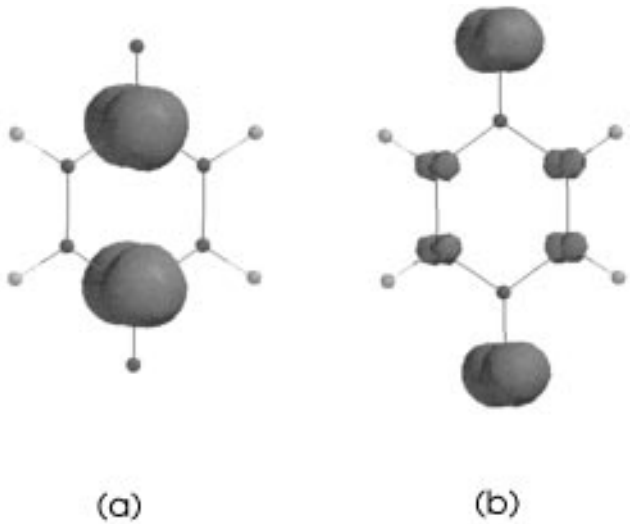

Figure 5. BQ^-/ETHANOL_A−BQ^- unpaired spin density difference plot contoured at (a) +0.0005 e/au^3 and (b) −0.0005e/au.^{3}

TABLE 2: BQ^- and BQ^-/ETHANOL_A (Parentheses): UB3LYP/EPR−II Calculated Hyperfine Couplings (MHz)

position	isotropic coupling A_{iso}	anisotropic coupling T_{11} T_{22} T_{33}	total coupling A_{11} A_{22} A_{33}
O	−20.1 (−21.0)	41.7 (37.7)	21.6 (16.7)
		41.1 (37.0)	21.0 (16.0)
		−82.9 (−74.5)	−103.0 (−95.5)
H	−6.5 (−6.1)	−3.4 (−3.4)	−9.9 (−9.5)
		−2.3 (−2.5)	−8.8 (−8.6)
		5.6 (5.8)	−0.9 (−0.3)
C_a	−10.3 (−3.6)	−8.2 (−12.5)	−18.5 (−16.1)
		−4.2 (−9.6)	−14.5 (−13.2)
		12.3 (22.0)	2.0 (18.4)
C_b	−0.3 (−1.6)	−7.0 (−6.4)	−7.3 (−8.0)
		−6.7 (−6.1)	−7.0 (−7.6)
		13.7 (12.5)	13.4 (10.9)
H(hb)	− (0.2)	− (6.4)	− (6.6)
		− (−3.2)	− (−3.0)
		− (−3.3)	− (−3.1)

bonded state. Relatively minor changes are brought about by changing the hydrogen-bonding solvent or the conformation of the hydrogen-bonded complex, a point which is emphasized by Table 3, where the total hyperfine tensor values for all complexes studied are given. As a result the ensuing discussion, as for the spin densities above, will focus on the comparison between BQ^- and BQ^-/ETHANOL_A principally because the largest body of experimental data exists for ethanol as solvent. The trends described below for the effects of hydrogen bonding on hyperfine couplings are similar for all solvents studied.

Comparing the hyperfine couplings for BQ^- and BQ^-/ETHANOL_A, Table 2, we can see that the isotropic and anisotropic hyperfine couplings for the ring hydrogen atom remain essentially unchanged on hydrogen bond formation with four ethanol molecules. Hydrogen bonding leads to a decrease in the absolute magnitude of the T_{33} anisotropic component of the ^{17}O coupling. The C_b and particularly the C_a ^{13}C couplings are particularly sensitive to hydrogen bonding. For C_b the principal change occurs for the isotropic coupling which decreases from −0.3 to −1.6 MHz on hydrogen bond formation, Table 2. The anisotropic couplings are relatively unchanged. For C_a, dramatic changes in both isotropic and anisotropic hyperfine couplings occur.

The isotropic (Fermi contact) arises from the presence of finite unpaired electron spin density at the nucleus. The unpaired electron is situated in a π type orbital (Figure 4), and hence unpaired electron spin density arises at the nuclear positions via spin polarization mechanisms.[13] The anisotropic couplings are, on the other hand, a direct measure of the dipolar interaction of the unpaired spin density with the nuclei. They are closely related to the spin density plots of Figure 4, with their magnitude being directly proportional to the concentration of spin and their symmetry (axial or rhombic) being determined by the distribution of this unpaired spin around the nucleus concerned. Previously in the absence of accurate molecular wave functions these anisotropic interactions have been explained by assuming that the π type molecular orbital near the nuclear positions can

TABLE 3: Comparison of Total Hyperfine Tensors for All Species: B Conformers in Brackets, All Values in MHz

position	water	methanol	ethanol	2-propanol
O	17.0(17.9)	16.7(17.2)	16.7(17.1)	(17.5)
	16.3(17.2)	16.0(16.4)	16.0(16.4)	(16.7)
	−96.4(−99.0)	−95.6(−98.1)	−95.5(−97.9)	(−98.7)
H	−9.6(−9.6)	−9.5(−9.5)	−9.5(−9.5)	(−9.6)
	−8.7(−8.7)	−8.6(−8.6)	−8.6(−8.6)	(−8.6)
	−0.3(−0.4)	−0.3(−0.3)	−0.3(−0.3)	(−0.4)
C_a	−16.3(−17.0)	−16.1(−16.6)	−16.1(−16.6)	(−16.9)
	−13.3(−13.7)	−13.2(−13.4)	−13.2(−13.4)	(−13.5)
	16.9(12.6)	18.4(14.6)	18.4(14.9)	(13.0)
C_b	−7.7(−7.7)	−8.0(−8.0)	−8.0(−7.9)	(−7.8)
	−7.4(−7.4)	−7.6(−7.6)	−7.6(−7.5)	(−7.4)
	11.9(11.9)	10.9(11.4)	10.9(11.4)	(11.7)
H(hb)	6.3(6.3)	6.6(6.4)	6.6(6.5)	(6.1)
	−2.7(−2.7)	−3.0(−3.0)	−3.0(−3.0)	(−2.8)
	−2.7(−2.7)	−3.1(−2.7)	−3.1(−2.8)	(−2.5)

be assumed to be of pure atomic p type.[13] For the oxygen atoms such a situation does indeed exist due to the nonbonding nature of the out of plane p functions on the oxygen atom (Figure 4). The anisotropic coupling of the oxygen atoms will be dominated by this large concentration of unpaired spin density. The cylindrical nature of the unpaired spin density concentrated around the O nucleus will as expected give rise to an axial anisotropic hyperfine coupling tensor. Hydrogen bond formation leads to a slight decrease in the anisotropic coupling of the oxygen atom. This can be directly correlated with a decrease in spin density at the oxygen atom on hydrogen bond formation shown in Figures 4 and 5 and discussed above.

For the C_a and C_b atoms the situation is somewhat different. Here a relatively low unpaired spin density compared with the O atom exists at both these atoms in the non-hydrogen-bonded state, Figure 4. Because of the imbalance in spin density between the O and C_a atom positions, the spin density near the O atom can be expected to contribute significantly to the anisotropic coupling of C_a. This is reflected in the rhombic symmetry of the C_a anisotropic coupling tensor for the non-hydrogen-bonded case as opposed to the axial tensor that would be expected from the atoms own π electron spin density. Hydrogen bond formation leads to a substantial change in the C_a ^{13}C anisotropic tensor principal values, Table 2. The tensor values are significantly increased, and the tensor assumes a more axial nature. This can be explained by reference to the spin density plots of Figures 4 and 5. The increased spin density at C_a on hydrogen bond formation leads to an increase in the anisotropic interaction for the C_a nucleus, and also the tensor assumes close to axial symmetry, reflecting the dominant contribution in this case of the spin density at the C_a position. For the C_b position an essentially axial anisotropic tensor is observed for both non-hydrogen-bonded and hydrogen-bonded cases. Here the distance from the O atom precludes any major contributions from this spin density to C_b's anisotropic coupling. The small decrease in coupling observed on hydrogen bond formation is a reflection of the decrease in spin density value demonstrated in Figure 5.

On the basis of the above analysis of the anisotropic couplings, it is now possible to discuss the trends in the isotropic couplings of Table 2. Such couplings are caused by spin density appearing directly at the nucleus in question. This arises due to spin polarization of the atom's s electrons by the unpaired π electron spin density.

The ^{13}C isotropic coupling for C_a and C_b are both negative in the non-hydrogen-bonded case, Table 2. This is a reflection of excess negative spin density at these nuclei. Spin polarization by the unpaired electron density of the atom's own p functions would be expected to contribute to excess of α spin leading to a positive isotropic coupling.[13] Spin polarization by the neighboring π α spin gives rise to excess β spin at the nuclear position, leading to a negative isotropic hyperfine coupling.[13] From the negative couplings observed, Table 2, it would appear that the polarization by the neighboring atoms predominates, giving rise to a negative isotropic hyperfine coupling for both carbon atoms. The larger negative coupling observed from the C_a position is a reflection of the enhanced spin polarization by the neighboring oxygen atom π spin density.

On hydrogen bond formation the ^{13}C isotropic coupling for C_a increases significantly, Table 2, and a small decrease in the magnitude of the C_b isotropic coupling is also observed. These can be directly related to the changes in anisotropic couplings referred to above. Increased spin density at C_a leads to an increased spin polarization by this spin density on the C_a s orbitals. This will increase the positive contribution to the isotropic coupling. The increased coupling value from −10.3 to −3.6 MHz is a consequence of this. For C_b the isotropic coupling is decreased in the hydrogen-bonded state, −0.3 to −1.6 MHz, Table 2. This reflects the slight decrease in π spin density at C_b, as shown in the spin density plots of Figure 5, leading to less positive contribution plus the increase in spin density at C_a, which increases the negative contribution to the C_b isotropic term. For the oxygen atom the isotropic coupling remains essentially unchanged after hydrogen bond formation. Here the decrease in spin density at the oxygen atom (leading via spin polarization to a decrease in the isotropic coupling) is counterbalanced by the increased spin density at C_a, which will lead to an increase in the ^{17}O isotropic coupling.

The above discussion has focused on BQ^-/ETHANOL_A, Figure 2. For the B conformer the hyperfine couplings calculated are very similar to the eclipsed form, Table 3. The only significant change is observed for the C_a atom position. For all B forms, Table 1, the hydrogen-bonding distance is larger than the A forms. The resultant weaker hydrogen bond can be expected to lead to a smaller redistribution of unpaired spin density from the O atom to the C_a position. This is indeed what is observed for the B conformers with the lower C_a spin density resulting in a lower anisotropic coupling for C_a and a lower isotropic coupling compared with the A forms.

(d) Comparison with Experimental Data. Extensive liquid solution studies of the *p*-benzosemiquinone anion radical were carried out in the 1960s.[14−16] ^1H, ^{13}C, and ^{17}O isotropic hyperfine couplings were determined in a wide range of solvents. The key finding of these studies was the decrease in the absolute magnitude of the ^{13}C C_a isotropic hyperfine coupling in hydrogen-bonding alcohol and water solvents, which is mirrored exactly by the findings of this study. In the 1980s powder ENDOR was used to obtain the ^1H isotropic and anisotropic hyperfine couplings in alcohol solvents.[17,18] For the ethanol solvent system the total hyperfine tensors have been determined for the ring and hydrogen bonding protons, and the isotropic values for the ^{17}O and ring carbons have been determined as well. For the proton data direct comparison with the total tensors of Tables 3 is possible. The experimental values reported for the principal hyperfine tensor of the hydrogen-bonded proton in an ethanol matrix are 5.9, −2.9, and −2.9 MHz.[17] These are in good agreement with the calculated values of Table 3. For the ring proton only two reliable principal hyperfine tensor values have been reported. These are −10.2 and −9.0 MHz, which are in excellent agreement with the calculated values of Table 2. The third tensor value is difficult to assign accurately due to a strong matrix ENDOR signal. It can be confidently attributed as being $<|1.0|$ MHz.[19] A situation such as this often occurs when analyzing powder ENDOR

spectra where one or more of the principal hyperfine tensor components is difficult to assign. The ability to be able to quantitatively predict the values of such tensors should be an invaluable aid to assignment. Identical values for the above tensors have also been reported for the 2-propanol solvent, showing good agreement with the values reported in Table 3.

EPR studies for the ethanol solvent system revealed ^{13}C isotropic values for the C_a and C_b positions of -3.3 and -1.2 MHz, respectively.[15] No ^{13}C anisotropic tensors for the *p*-benzosemiquinone radical have been reported. These show impressive agreement with the calculated values of -3.6 and -1.6 MHz of Table 2. The ^{17}O isotropic value determined in an ethanol solvent is -24.4 MHz.[16] This again is in good agreement with the calculated value of -21.0 MHz in Table 2. An A_{33} value of -91.5 MHz has also been reported[20] for this radical, which is again in good agreement with the -95.5 MHz value of Table 2.

Conclusions

Density functional calculations using the B3LYP functional have shown that the unpaired spin density distribution of the *p*-benzosemiquinone anion radical is altered significantly on hydrogen bond formation with alcohol solvent molecules. In essence, hydrogen bonding leads to a redistribution of the unpaired spin density from the O to the C_a position. Calculated anisotropic and isotropic hyperfine coupling constants are shown to reflect such a redistribution, which is confirmed by experimentally determined hyperfine couplings obtained in various solvent systems. Variation of the alcohol solvent or the conformation of the hydrogen-bonding interaction leads to only minor changes in calculated spin densities and hyperfine coupling constants. The ability to obtain quantitatively accurate hyperfine coupling constants using the B3LYP functional combined with the EPR-II basis set is clearly demonstrated and should be used in the future to aid the assignment of EPR and ENDOR spectra.

The changes in spin density noted for this model semiquinone system can now be used as a foundation to provide further insight into the electronic consequences of hydrogen bonding for in vivo semiquinones.

References and Notes

(1) *Functions of Quinones in Energy Conserving Systems*; Trumpower, B. L., Ed.; Academic Press: New York, 1986.

(2) Okamura, M. Y.; Feher, G. *Annu. Rev. Biochem.* **1992**, *61*, 861.

(3) van den Brink, J. S.; Spoyalov, A. P.; Gast, P.; van Liemt, W. B. S.; Raap, J.; Lugtenburg, J.; Hoff, A. J. *FEBS Lett.* **1994**, *353*, 272.

(4) Breton, J.; Burie, J.-R.; Boullais, C.; Berger, G.; Nabedryck, E.; Mioskowski, C. *Biochemistry* **1994**, *33*, 14378.

(5) van Liemt, W. B. S.; Boender, G. J.; Gast, P.; Hoff, A. J.; Lugtenberg, J.; de Groot, H. M. J. *Biochemistry* **1995**, *34*, 10229.

(6) Adamo, C.; Barone, V.; Fortunelli, V. *J. Chem. Phys.* **1995**, *102*, 1689.

(7) O'Malley, P. J.; Ellson, D. A. *Chem. Phys. Lett.* **1996**, *260*, 492.

(8) O'Malley, P. J. *Chem. Phys. Lett.* **1996**, *262*, 797. O'Malley, P. J. *J. Phys Chem.*, submitted for publication.

(9) Barone, V. In *Recent Advances in Density Functional Methods*; D. P. Chong, Ed.; World Scientific Publishing: Singapore, 1995.

(10) Becke, A. D. *J. Chem. Phys.* **1993**, *98*, 5648.

(11) Frisch, M. J.; Trucks G. W.; Schlegel, H. B.; Gill, P. W.; Johnson, B. G.; Wong, M. W.; Foresman, J. B.; Robb, M. A.; Head-Gordon, M.; Replogle, E. S.; Gomperts, R.; Andres, J. L.; Raghvachari, K.; Binkley, J. S.; Gonzalez, C.; Martin, R. L.; Fox, D. J.; Defrees, D. J.; Baker, J.; Stewart, J. J. P.; Pople, J. A. *GAUSSIAN 94*; Gaussian Inc.: Pittsburgh, PA, 1995.

(12) *SPARTAN 4.1.1*; Wavefunction Inc.: California, 1995.

(13) Gordy, W. *Theory and Applications of Electron Spin Resonance*; Wiley: New York, 1980.

(14) Das, M. R.; Venkataraman, B. *J. Chem. Phys.* **1965**, *42*, 1320.

(15) Gendell, J.; Freed, J. H.; Fraenkel, G. K. *J. Chem. Phys.* **1962**, *37*, 2832.

(16) Gulick, W. M.; Geske, D. H. *J. Am. Chem. Soc.* **1966**, *88*, 4119.

(17) O'Malley, P. J.; Babcock, G. T. *J. Am. Chem. Soc.* **1984**, *106*, 817.

(18) O'Malley, P. J.; Babcock, G. T. *J. Am. Chem. Soc.* **1986**, *108*, 3995.

(19) Burghauss, O.; Plato, M.; Rohrer, M.; Mobius, K.; MacMillan, F.; Lubitz, W. *J. Phys. Chem.* **1993**, *97*, 7639.

(20) Macmillan, F.; Lendzian, F.; Lubitz, W. *Magn. Reson. Chem.* **1995**, *33*, 581.